Metal- and Halogen- free Synthesis of Ordered Mesoporous Carbon Materials

Farzeen Sakina, Richard T. Baker*

EaStChem School of Chemistry, University of St Andrews, St Andrews, Fife, United Kingdom KY16 9ST

Abstract

Mesoporous carbon materials are of great interest as catalyst supports. However, the presence of impurities such as the metal or halide ions which are often used to catalyse the polymerisation and condensation reactions in their preparation can be poisonous to the final catalyst product. For this reason, in this work, metal- and halogen-free mesoporous polymer and carbon materials (OMCs) were synthesised using a modified two phase method employing alternative polymerisation and condensation catalysts. The OMC materials synthesised exhibit a highly ordered two dimensional hexagonal arrangement of cylindrical mesopores, as revealed by small angle XRD, gas physisorption and TEM analysis, and have typical specific surface areas of ca. 600 m^2/g, pore size of ca. 7.0 nm, and pore volume of approximately 0.60 cm^3/g. Their physical evolution with increasing calcination temperature is examined as are the effects of varying synthesis parameters on the nature of the final mesostructure.

Keywords: Ordered, Mesoporous, Carbon, Catalyst Support, Calcination

***Corresponding author.** E: rtb5@st-andrews.ac.uk; T: +44 1334463899

1. Introduction

Due to their potential applications in various fields such as catalysis, gas separation, electrochemistry and energy storage, ordered mesoporous carbons (OMCs) have been extensively studied since their first discovery in 1999[1,2,3]. OMCs were first synthesised by Rayoo et al. in 1999 by nanocasting. This method involved impregnation of pre-synthesized silica templates with a carbon precursor, carbonisation and template removal, usually by dissolution in NaOH or HF. The resulting mesoporous carbons were inverse replicas of the mesoporous silica templates. The time required and cost of synthesising hard templates are major drawbacks of this method, however. Furthermore, the high-temperature treatment and the reaction with NaOH or HF required to remove the hard template can affect the final structure of the OMC product[1,4,5,6,7]. An alternative to nanocasting is the soft templating synthesis of OMCs involving organic-organic self- assembly of carbon precursors, usually phenol-formaldehyde resins, and a structure directing agent such as the block copolymers, F127 and P123. A range of synthetic routes such as evaporation induced self- assembly (EISA) [8], an aqueous route[6] and phase separation[3] have been reported. Each of these has its own advantages and disadvantages. In the EISA method, the cooperative assembly of carbon precursors and the template occurs during evaporation of solvent, and a family of highly ordered mesoporous carbon materials can be made including 2-D hexagonal (FDU-15), 3-D bi-continuous (FDU-14), body-centred cubic (FDU-16) and lamellar mesostructures[8]. However, this method is not suitable for large scale production due to the requirement to evaporate a large amount of organic solvent[3,9]. The dilute aqueous route utilises hydrogen bonding to drive the cooperative self-assembly in aqueous media. In 2005, Zhao et al. first reported this method for the direct synthesis of a novel bi-continuous cubic mesoporous polymer (FDU-14) and carbon (C-FDU-14) with *Ia3̄d* symmetry. With this method, OMCs with controllable pore sizes and various morphologies could be made. The main drawback of this process is the narrow pH window (around 9.0) of the reaction since higher pH results in weakening of the hydrogen bonding while neutral or acidic media slow the rate of polymerisation[10]. Hydrothermal autoclaving methods have been used to make OMCs but these are limited by the high energy consumption needed to attain the high temperature and pressure required[11]. Dai et al developed an acid-catalysed two phase method which is simple, practicable and scalable[12]. However, this process requires strongly acidic conditions for the reaction. Another base-catalysed two phase method developed by Zhang et al. produced highly ordered mesoporous carbon material. This method is highly effective in terms of scalability, reproducibility and simplicity[3]. Furthermore,

in the basic medium the cross-linking within the phenolic resins increases resulting in more stable structures after calcination[8,13]. The only drawback of this method is the use of inorganic catalysts containing metal and halogen ions which is undesirable for certain applications such as catalysis.

Phenolic resins are typically used as carbon precursors for OMC synthesis. These contain three dimensional networks in which polymer chains are linked together in all directions via crosslinks. Undesirably brittle products are obtained if too many cross-links are formed[14]. To avoid this, these resins are prepared in two stages. In the first stage phenol and formaldehyde (F) are polymerised to form a processable intermediate (soluble and fusible) called resol (base catalysed) or novolak (acid catalysed). In the second stage this processable intermediate is condensed to the final cross-linked product using an acid catalyst or simplly by heating[14]. In order to make mesoporous material, this condensation must occur in a solution containing a structure directing agent such as F127. A schematic representation of the overall procedure is given in **Fig. 1**.

Herein we report a metal- and halogen-free synthesis of OMCs adapted from an original two phase method developed by Zhang et al[3]. Ammonium hydroxide (NH_4OH) and oxalic acid were used to catalyse the polymerisation and condensation reactions, respectively, of resorcinol (R) and formaldehyde (F). When NH_4OH is used as a catalyst for polymerisation of R with F, it should be added after at least 1 h of mixing otherwise an insoluble compound is formed[15,16]. Therefore, the first step in this synthesis is oligomerisation without catalyst (NH_4OH) for a certain period of time, t_o, and at temperature, T_o (**Fig. 1i**). The second step is polymerisation catalysed by NH_4OH for time, t_p, at temperature, T_p, to form the resorcinol-formaldehyde polymer known as RF resol (**Fig. 1ii**). This RF resol is then mixed with a solution of Pluronic F127 which acts as a template or structure-directing agent. Oxalic acid is then added to catalyse condensation of the RF resol and organic-organic self-assembly to form a mesostructured material (**Fig. 1iii**). This is marked by phase separation and after drying the resulting gel the F127 template is removed by heating under nitrogen to form the OMC. The effect of various synthesis parameters on the properties of the final mesostructure, such as t_o, T_o, t_P, T_p and amount of NH_4OH added (C_{NH4OH}) were also studied in this paper.

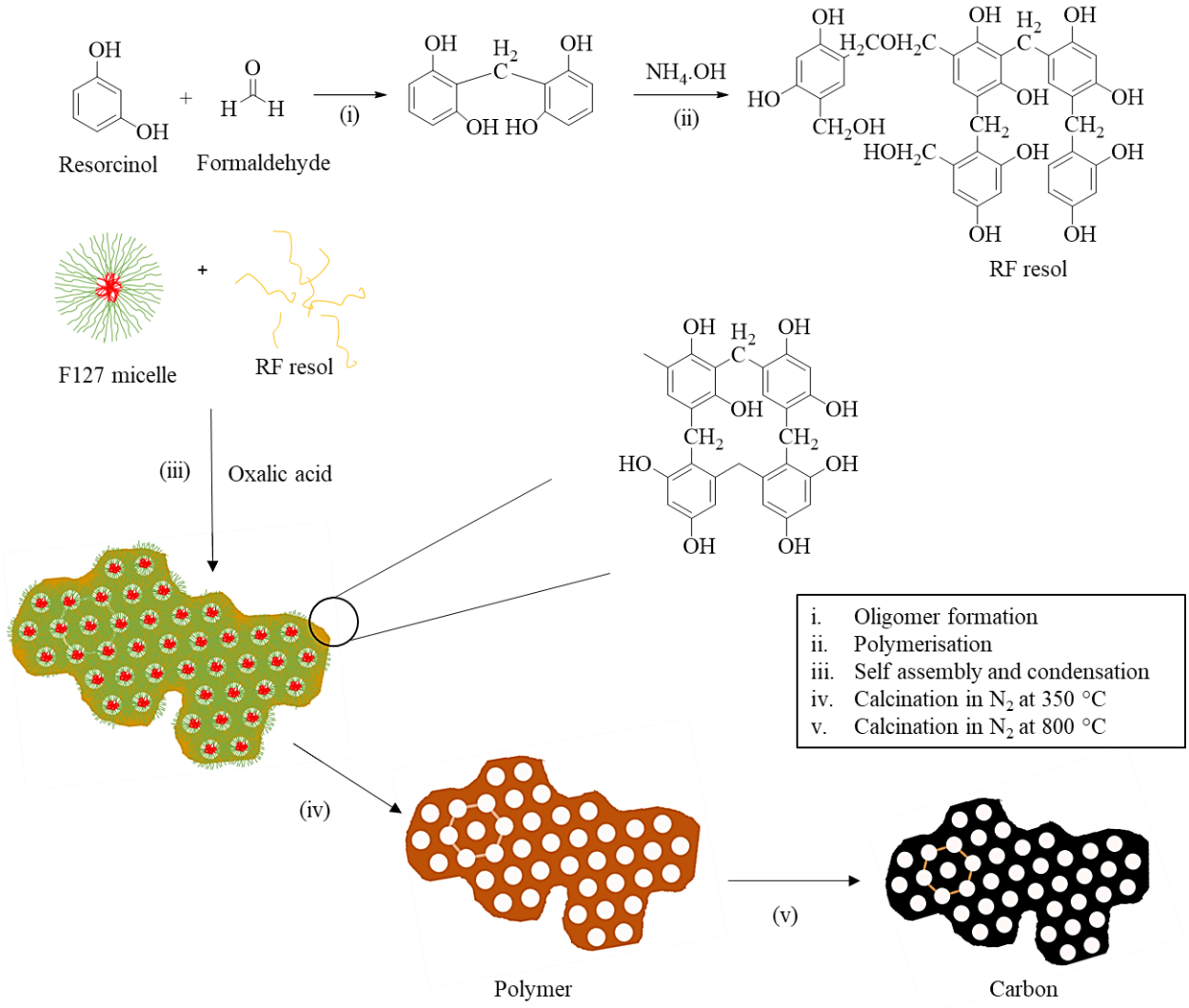

Fig. 1 - Schematic diagram of NH_4OH-catalysed resorcinol-formaldehyde resin formation in the preparation of OMC materials.

2. Experimental Section

2.1. Chemicals

Pluronic F127 and resorcinol (99 %) were purchased from Sigma Aldrich. Formaldehyde (37 %) and Absolute Ethanol were purchased from VWR. Ammonia solution (35 %) was purchased from Fisher Scientific and Oxalic acid (98%) was purchased from Alfa Aesar. All chemicals were used as received without purification. Millipore water was used in all experiments.

2.2. Synthesis Procedure

The 2D hexagonal OMCs were prepared using a two phase method with molar ratios of the reagents, resorcinol/formaldehyde/F127/NH_4OH/oxalic acid = 1:1.39:0.00635:0.01:0.125. In a typical procedure, a precursor solution of resorcinol and formaldehyde is made by mixing 2.20 g of resorcinol with 2.26 g of 37 wt% formaldehyde solution for 1 h at 35 ºC. 2 ml of 0.1M NH_4OH was added and the solution was stirred for a further 1 h to obtain RF resol. This RF resol was cooled to 18 °C for 10 min. and was mixed with a solution containing 1.60 g of F127, 8 g of water and 10 g of ethanol for 20 min. 0.225g of oxalic acid was added with continuous stirring. After 5-10 min., the clear solution became cloudy indicating phase separation. After constant stirring for a further 1 h, the mixture was left standing overnight to obtain the polymer gel phase. This polymer gel was dried for at least 12 h at room temperature and cured at 80 ºC for 24 h. The resultant material was finally carbonised at temperatures ranging from 350 to 1200 °C for 3 h with a heating rate of 1ºC min^{-1} under flowing N_2 atmosphere (100 cm^3 min^{-1}) to obtain the OMC products.

2.3. Characterisation

Gas physisorption analysis was carried out on the OMC products using a Micrometrics TriStar II 3020 using liquid N_2 at 77K. Samples were degassed at 120 ºC under vacuum for at least 12 h. Micrometrics software was used to calculate Brunauer–Emmett–Teller (BET) specific surface areas and the Barrett, Joyner and Halenda (BJH) pore size distribution from the adsorption branches of the isotherms. Small angle XRD (SAXRD) patterns were recorded using a PANalytical Empyrean diffractometer in reflectance geometry using Cu Kα radiation. Transmission Electron Microscopy (TEM) was carried out using a JEOL JEM 2011 instrument operating with a LaB6 filament at an accelerating voltage of 200 kV. TEM samples were prepared by suspending the ground mesoporous sample in acetone by ultrasonication for 1 min, sweeping a 300-mesh holey carbon TEM grid through the suspension and allowing this to dry under a halogen lamp overnight. The FT-IR experiments were performed using a Shimadzu IRAffinity-1S Fourier Transform infrared spectrophotometer with high-performance LabSolutions IR software. The spectra were recorded from 4000 to 400 cm^{-1} . A background spectrum was taken before each measurement. Solid-state ^{13}C NMR spectra were recorded on a Bruker Avance III spectrometer equipped with a 9.4 T wide-bore superconducting magnet (^1H and ^{13}C Larmor frequencies of 400.1 and 100.6 MHz, respectively). Samples were packed into 4 mm zirconia rotors and rotated at the magic angle at a rate of 12.5 kHz. Spectra were recorded with cross polarisation (CP) from ^1H using a spin-lock pulse (ramped for ^1H) of 3.5

ms. Signal averaging was carried out for between 1024 and 10240 transients with a recycle interval of 5 s. High-power (v~100 kHz) ^{1}H TPPM-15 decoupling was applied during acquisition. In the Temperature Programmed Oxidation (TPO) experiments, 70 mg of sample was placed on a porous quartz frit in a quartz micro-reactor. The micro-reactor was placed in a small oven and purged under Ar to remove air and moisture (about 10 min). The TPO experiment was then performed by heating the sample from ambient temperature to 800 °C at a rate of 10 °C /min under a flow of dry 5% O_2/Ar. The outlet gas from the microreactor was analysed in real time using a quadrupole mass spectrometer (Cirrus 2). The variation in up to sixteen mass to charge ratios, *m/q*, were recorded including *m/q* = 28 (CO), 32 (O_2) and 44 (CO_2) and these were plotted against sample temperature to generate the TPO plots.

3. Results and Discussion

3.1. Synthesis of OMCs and effect of Calcination Temperature

After curing at 80 °C for 24 h, the mesostructured intermediate material made using NH_4OH and oxalic acid catalysts was calcined at calcination temperature, T_{calc}, of 300, 350, 400, 500, 600, 800, 1000 or 1200 ºC. The SAXRD patterns of the samples calcined at 350-1200 ºC show three well-resolved diffraction peaks that could be indexed as reflections from the 100, 200 and 210 planes of the two-dimensional hexagonal mesopore structure (**Fig. 2a**). The sample calcined at 300 ºC showed only a very weak peak corresponding to the 100 plane. On increasing T_{calc}, there was a general decrease in the d-spacings and unit cell parameters of the pore structure (**Fig. 2b and Table 1**) which indicates the contraction of the mesoporous framework upon calcination. The presence of three peaks in the sample calcined at 1200 ºC shows the stability of the pore structure of these materials even after treatment at very high temperature.

TEM images of particles of the samples calcined at 350 °C (**Fig. 3 a-c**) and 400 °C (**Fig 3 d-f)** indicate the presence of cylindrical mesopores in a 2-D hexagonal arrangement viewed along the [110] and [001] directions, respectively. The highlighted hexagon in **Fig. 3f** shows that the pore itself has hexagonal cross-section indicating the *p6mm* symmetry of these OMCs. The presence of long range order in the sample calcined at 1200 ºC (**Fig. 3 g-i**) is in agreement with the SAXRD results in showing a highly ordered 2D arrangement of pores which is stable to high temperatures.

The N_2 physisorption data for the samples calcined at different temperatures are given in **Fig. 4, 5** and **Table 1**. In **Fig. 4a** all samples show a Type IV isotherm with a sharp capillary condensation step at relative pressure, 0.4 - 0.8, and an H1 type hysteresis loop which indicates

the presence of cylindrical mesopores. The isotherm of the sample calcined at 300 ºC (**Fig. 4a**) showed by far the lowest adsorption and had the lowest value of specific surface area (7 m^2/g), pore volume (0.02 cm^3g) and micropore volume (0 cm^3g). This indicates that this temperature is not high enough for effective template removal. At T_{calc} = 350 ºC, there was a sharp increase in all of these parameters which represents the removal of the template **(Fig. 5 and Table 1)**. Upon further calcination, the pore volume decreased while the micropore volume increased smoothly. The specific surface area increased till T_{calc} = 600 ºC and then decreased (**Table 1)**. The adsorption and desorption branches of the isotherms of the samples calcined at 350 ºC and 400 ºC are not closed (**Fig. 4a**). This indicates their polymeric nature as this behaviour is mostly attributed to the swelling of the polymer matrix during the physisorption experiment[17]. **Fig. 4b** shows that all samples had narrow pore size distributions (PSD) and that, as T_{calc} increased, the position of the maxima in PSD shifted smoothly to lower values, this shift becoming gradually smaller until at T_{calc}=1000 °C and 1200 °C, the maxima are in almost the same position. It can be seen from **Table 1** that besides pore diameter, wall thickness also decreased with increasing T_{calc}. This indicates the contraction of the polymer framework due to increased degree of condensation of the phenolic resin[8]. At 800 ºC the conversion of the polymeric framework to carbon seems to have been almost complete and further increase in temperature had less effect on these parameters.

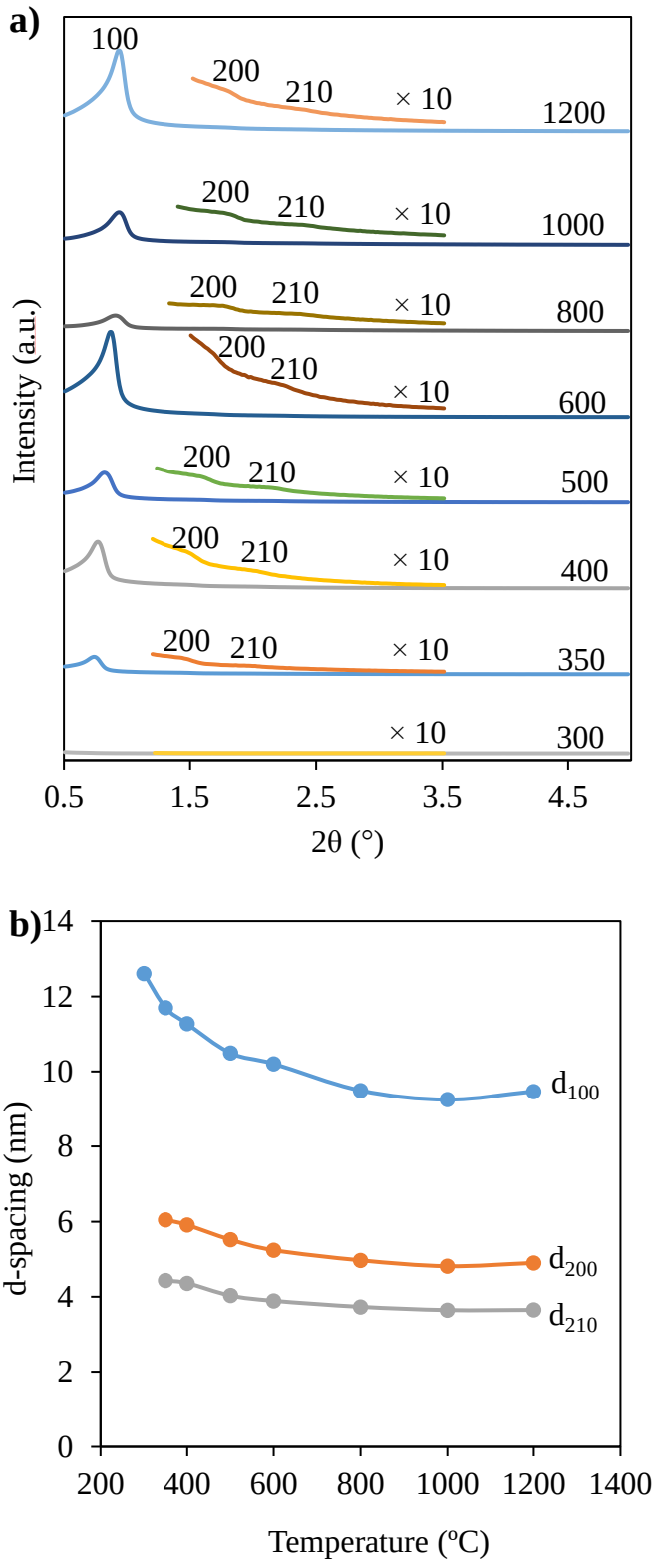

Fig. 2 - (a) SAXRD patterns and (b) d-spacing data for mesoporous samples calcined at the temperatures indicated in the figure .

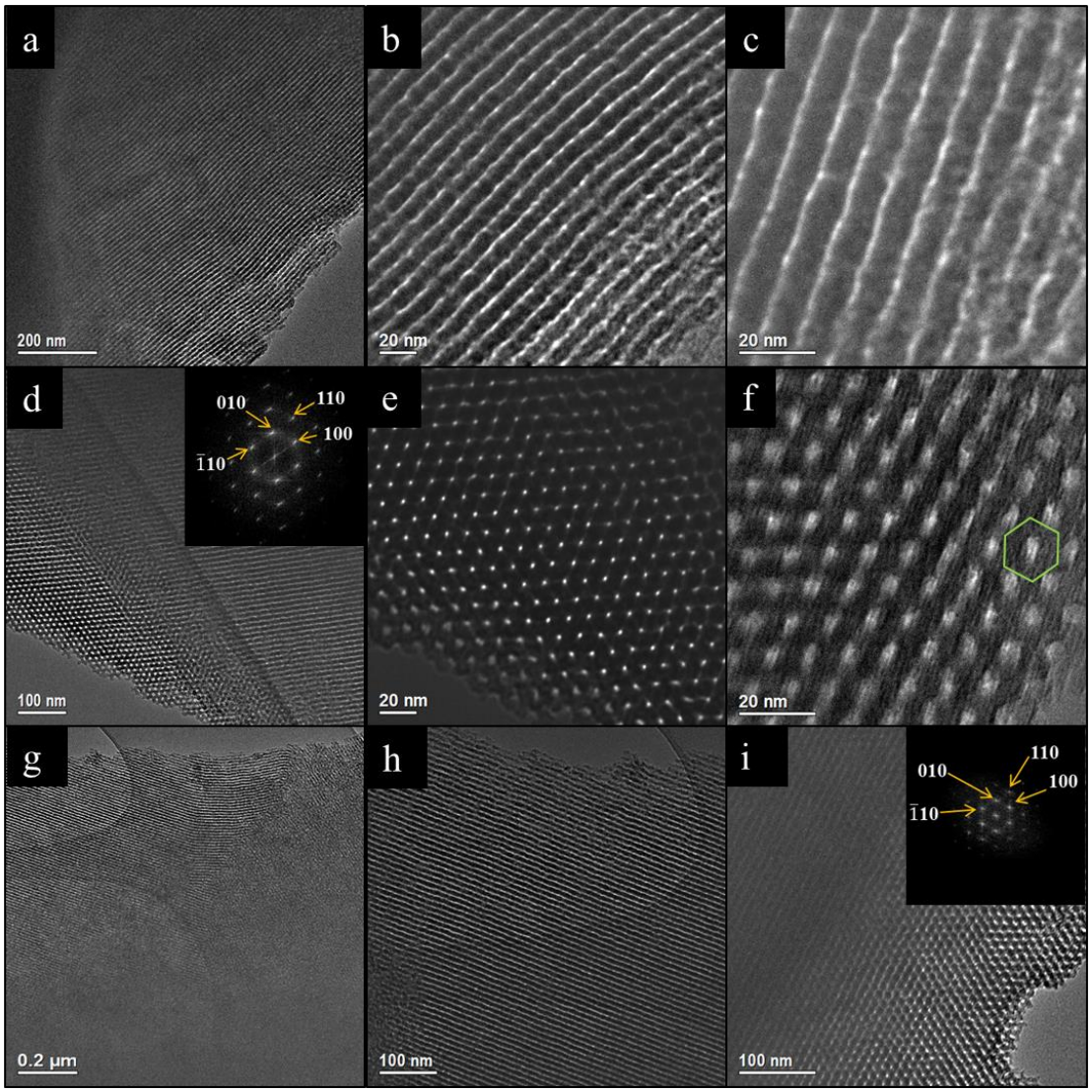

Fig. 3 - Low, medium and high magnification TEM images of samples calcined at: (a-c) 350 °C, (d-f) 400 °C, and (g-i) 1200 °C. DDPs are inset in (d) and (i).

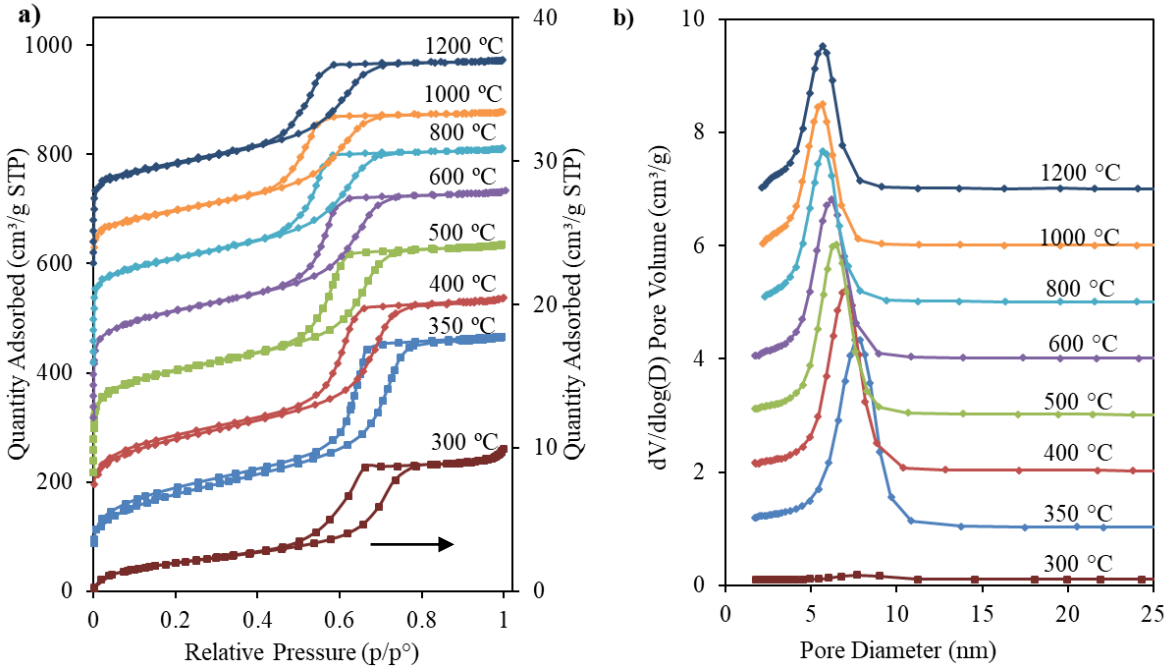

Fig. 4 - a) Nitrogen sorption isotherms; and (b) pore size distributions of ordered mesoporous carbons calcined at the temperatures indicated in the figure. Plots are shifted on the y-axis in steps of 100 cm^3/g in (a) and 1 cm^3/g in (b) for clarity. The isotherm for the sample calcined at 300 °C is plotted on a secondary axis.

The FT-IR spectra of the samples calcined at different temperatures are given in **Fig. 6**. For T_{calc} = 300 ºC the IR bands are most intense. Those between 1300 and 1000 cm^{-1} may be assigned to the in-plane bending of the aromatic ring C-H bonds[18]. The bands at 1609 and 1445 cm^{-1} are due to C-C stretching in the aromatic rings and bands around 1100 cm^{-1} and at 2868 cm^{-1} correspond, respectively, to the C-O and C-H stretch in the phenolic resin and F127 template [19188]. A weak broad band around 3468 cm^{-1} indicates the presence of the OH group[18]. The intensities of all these bands decreased as the calcination temperature increased and almost disappeared above T_{calc}=600 ºC. This indicates the gradual removal of F127 and conversion of mesoporous polymer to mesoporous carbon through progressive loss of functional groups.

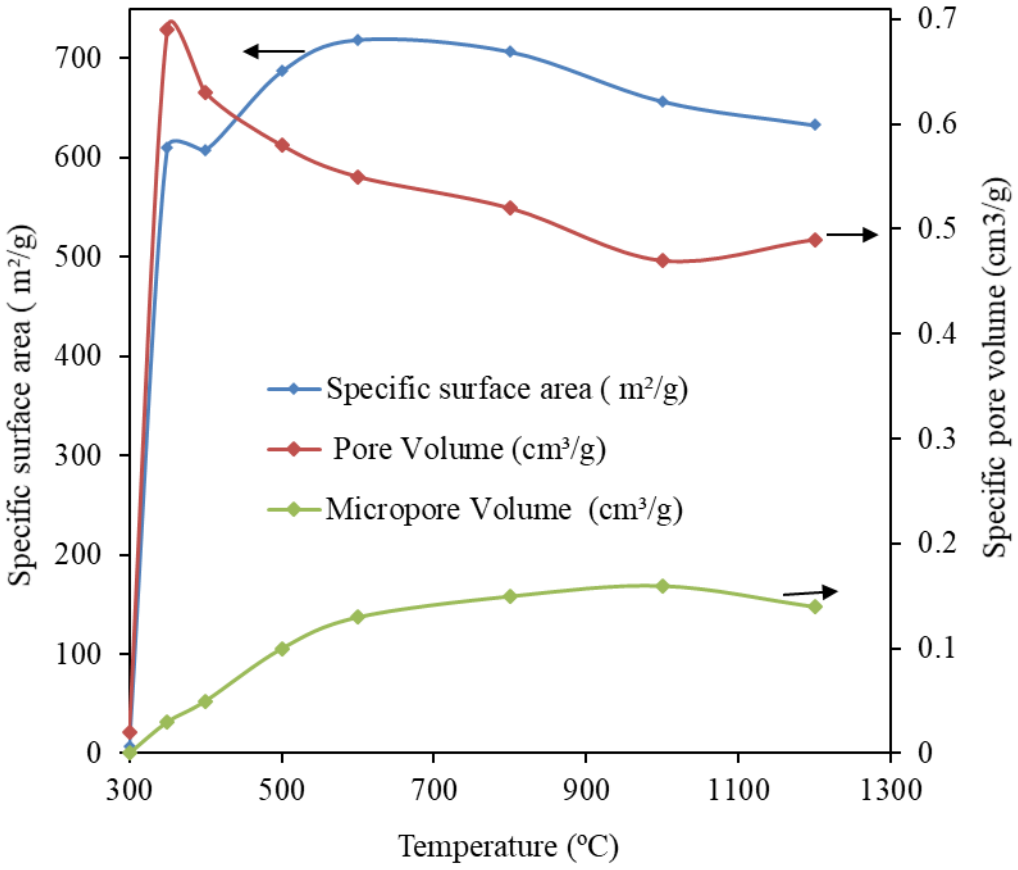

Fig. 5 - Specific surface area, micro- and mesopore volume as a function of calcination temperature.

Table 1 - Physisorption and XRD data of OMCs calcined at the temperatures indicated.

Temperature (ºC)	SSA (m^2/g)	V_P (cm^3/g)	V_{micro} (cm^3/g)	D_p (nm)	a (nm)	W_T (a-D_p)
300	7	0.02	0.000	8.0		
350	610	0.69	0.034	7.7	13.5	5.8
400	608	0.63	0.053	7.0	13.0	6.0
500	687	0.58	0.103	6.3	12.1	5.8
600	719	0.55	0.134	6.2	11.8	5.6
800	707	0.52	0.153	5.7	11.0	5.3
1000	657	0.47	0.160	5.6	10.7	5.1
1200	633	0.49	0.140	5.7	10.9	5.2

SSA: Specific surface area; V_P: Pore volume; V_{micro}: Micropore volume; D_P: Pore diameter; a: Unit cell parameter = ($2d_{100}/\sqrt{3}$); W_T: Wall thickness (a-D_P)

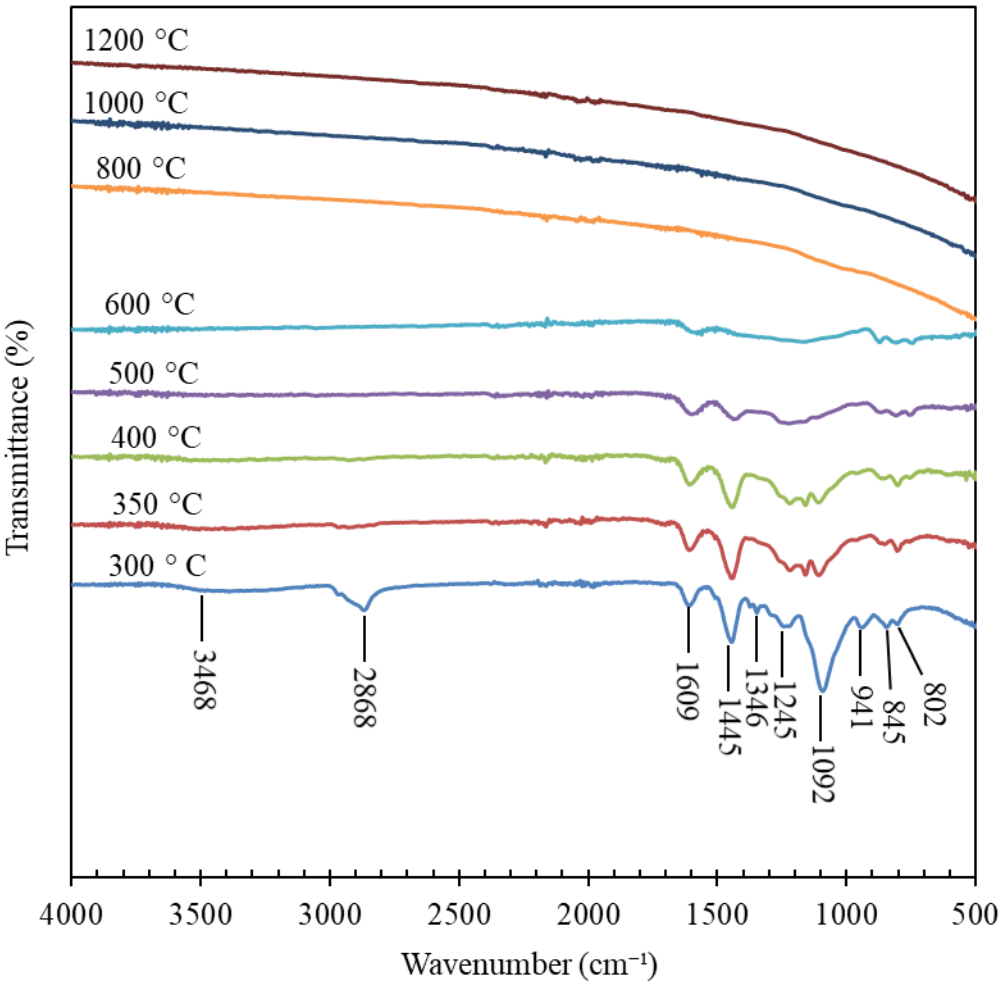

Fig. 6 - FT-IR spectra of ordered mesoporous carbons calcined at the temperatures indicated in the figure. The plots are shifted on the y-axis for clarity.

The ^{13}C cross-polarization magic angle spinning (CP-MAS) NMR spectra of the samples calcined at different temperatures are given in **Fig. 7**. It can be seen that the sample calcined at 300 °C contained an intense and narrow peak around 70 ppm which corresponds to the structure-directing agent, F127. This indicates that this temperature is not enough for the removal of the F127. By further increasing the temperature to 350 °C, only traces of F127 remained. On increasing the T_{calc}, the number of OH groups decreased as evident by the reduction in the relative amount of signal at ~ 152 ppm, assigned to C1. At 800 °C, the signal was very poor even after averaging for 10240 transients with a full rotor of material, suggesting that the material is essentially elemental carbon (since in a CP experiment, the initial magnetisation is generated on ^{1}H and transferred to ^{13}C). The ratio of the integrated spectral

intensity between 162 and 140 ppm to that between 140 and 98 ppm, corresponding (roughly) to the relative C(OH): CH ratio is plotted in **Fig. 8**. This clearly shows a progressive loss of OH groups with temperature.

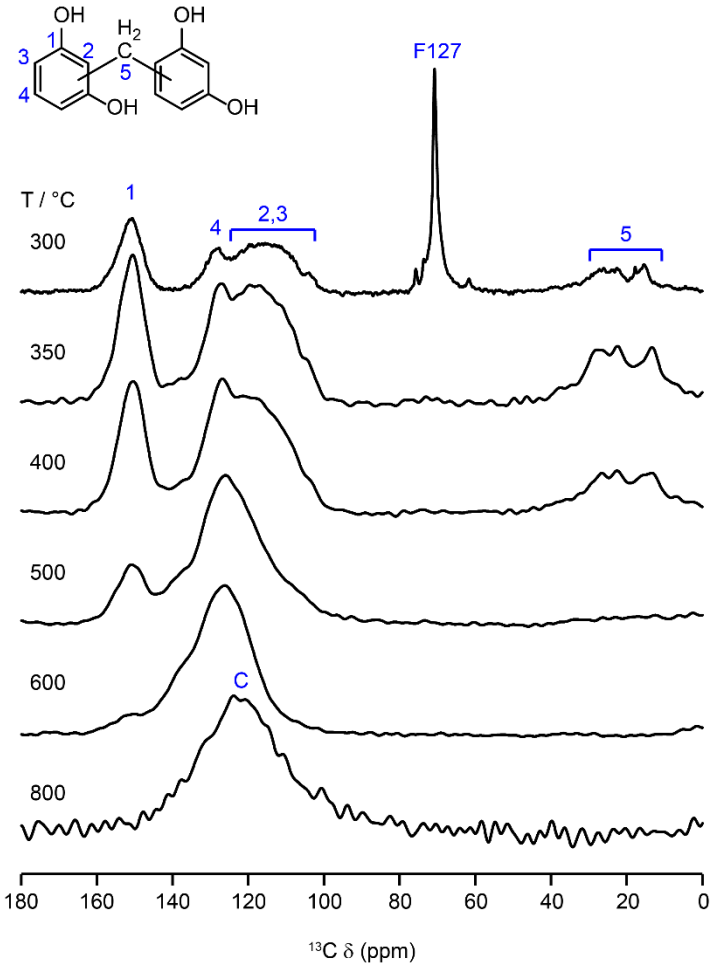

Fig. 7 - ^{13}C (9.4 T, 12.5 kHz CP MAS) NMR spectra samples of mesostructured carbon materials calcined at the temperatures indicated on the figure. Spectral assignments follow the numbering scheme shown and are based on previous assignments of Meng et al [18].

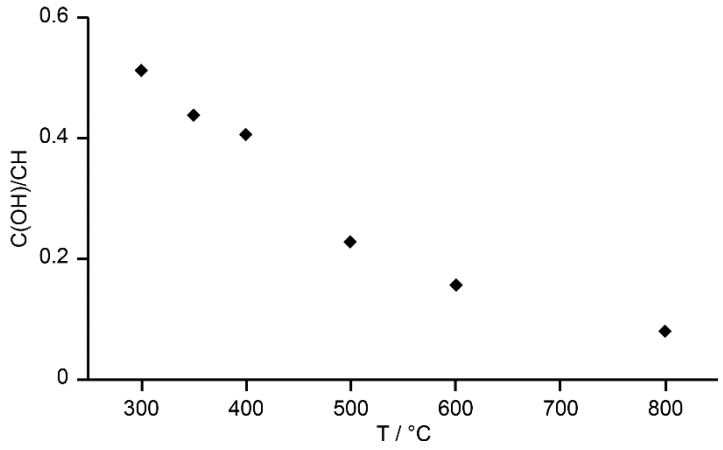

Fig. 8 - Plot of the integrated intensity of the C1: C2+C3+C4 resonances (integral regions of 162-140 ppm and 140-98 ppm, respectively) as a function of sample calcination temperature.

TPO experiments were performed to study the thermal stability of the mesoporous carbon samples calcined at temperatures ranging from 350 to 1200 °C. The results are presented in terms of CO_2 production on reaction of carbon species in the sample with gas phase oxygen and are plotted in **Fig. 9**. The samples calcined at 350-500 °C showed a peak at T_1 (roughly 400 °C), indicating the presence of reactive functional groups in these samples. This peak was absent in samples calcined above 500 °C indicating the loss of what might be termed organic material in samples calcined at higher temperatures. The peaks at T_2 and T_3 were present in all samples and can be assigned to condensed polymeric material. The position of these peaks shifted to higher temperature with increasing T_{calc}. This indicates the increased degree of functional group loss, condensation and carbonisation with increasing T_{calc} since the resulting structure is more stable to oxidation than the polymeric structure.

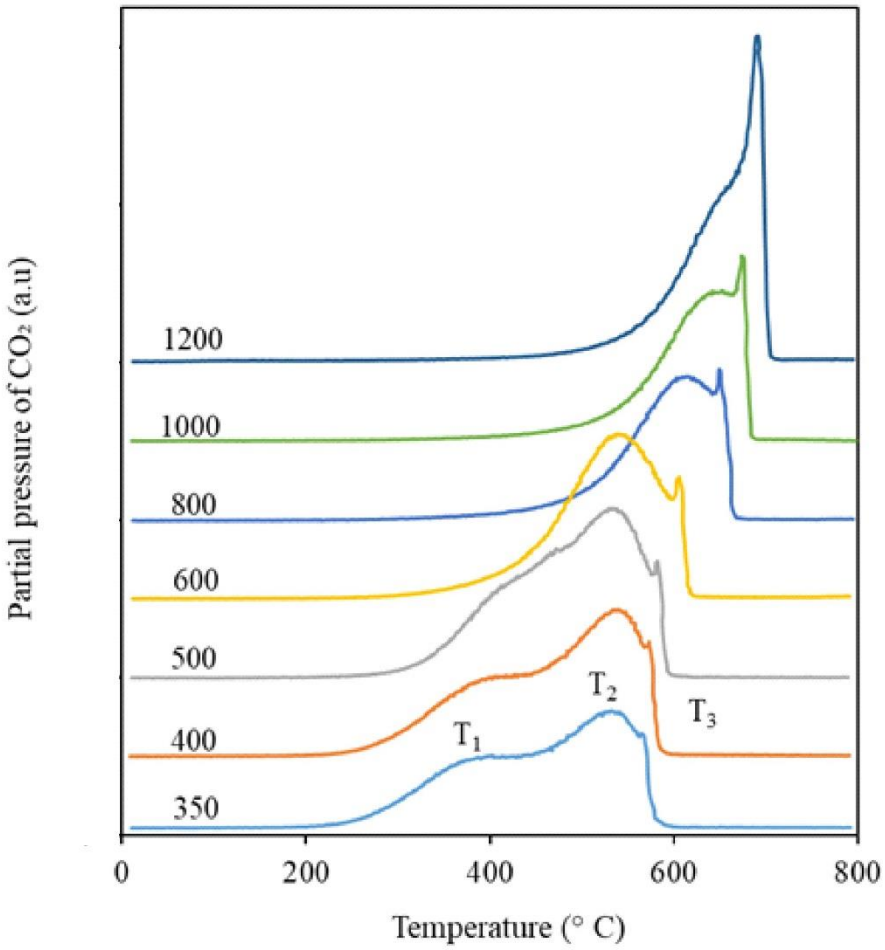

Fig. 9 - CO_2 traces obtained in the TPO experiments performed on ordered mesoporous carbons calcined at the temperatures indicated on the figure (in °C). Plots are shifted on the y-axis for clarity.

3.2 Scalability

Fig. 10a and **b** show the SAXRD patterns and N_2 physisorption isotherms (with pore size distributions inset), respectively, of the samples prepared at two different scales, the scale used in the previous section and a preparation of 25 times the quantity of product. The SAXRD pattern of the sample prepared on the large scale is similar to the sample prepared on the small scale and both correspond to a highly ordered 2D hexagonal mesostructure. The physisorption isotherm and pore size distributions of the two samples are also almost identical (**Fig. 10b**). The samples show very close values of specific surface area, (605 and 608 m^2/g), pore volume (0.61 and 0.63 cm^3/g) and micropore volume (both 0.05 cm^3/g). The PSDs of both samples have maxima at pore diameters of 7.0 nm and very similar d-spacings of 11.4 and 11.3 nm.

These results indicate that this method is scalable and that such OMC materials can be prepared in big batches.

3.3 Factors affecting final mesostructure

3.3.1. Effect of T_o

To investigate the effect of oligomerisation temperature (T_o) on final mesostructure, experiments were performed in which T_o was set to 18 °C or 35 °C, keeping all other reaction parameters constant. The SAXRD patterns of both samples (**Fig. 11a**) show the three peaks typical of a highly ordered two dimensional hexagonal mesostructure. Nitrogen adsorption isotherms and pore size distributions are given in **Fig. 11b**. It can be seen that samples T_o=18 and 35 °C both showed typical Type IV isotherms and H1 hysteresis loops characteristic of cylindrical mesopores (**Fig. 11b**) as well as narrow pore size distributions centred at 6.8 and 6.9 nm, respectively (**inset Fig. 11b**). The samples had very close values of specific surface area (605 and 608 m^2/g) and pore volume (0.61 and 0.63 cm^3/g) and the same micropore volume (both 0.05 cm^3/g). These results indicate that changing T_o did not noticeably affect the final mesostructure.

3.3.2. Effect of t_o

In this synthesis, oligomerisation time, t_o, is typically 1 h. In order to find whether a further increase in t_o would have an effect on the final mesostructure, a preparation was performed with t_o = 2 h. All other synthesis parameters were kept the same.

As can be seen in **Fig. 12a** the SAXRD patterns of the samples made with t_o = 1 h and t_o = 2 h are similar and both show three peaks corresponding to highly ordered two-dimensional hexagonal mesostructures. The specific surface area, pore volume and micropore volume of the sample made using t_o = 2 h were found to be 600 m^2/g, 0.61 cm^3/g and 0.05 cm^3/g respectively which are very close to the values of 608 m^2/g, 0.63 cm^3/g and 0.05 cm^3/g obtained with t_o = 1 h. The isotherms of both samples match and both have a Type IV profile with H1 type hysteresis loops indicating cylindrical mesopores (**Fig. 12b**). The samples had similar pore size distributions with maxima centred at 7.0 nm (inset in **Fig. 12b**). These results indicate that increasing t_o to 2 h does not significantly affect the final mesostructure.

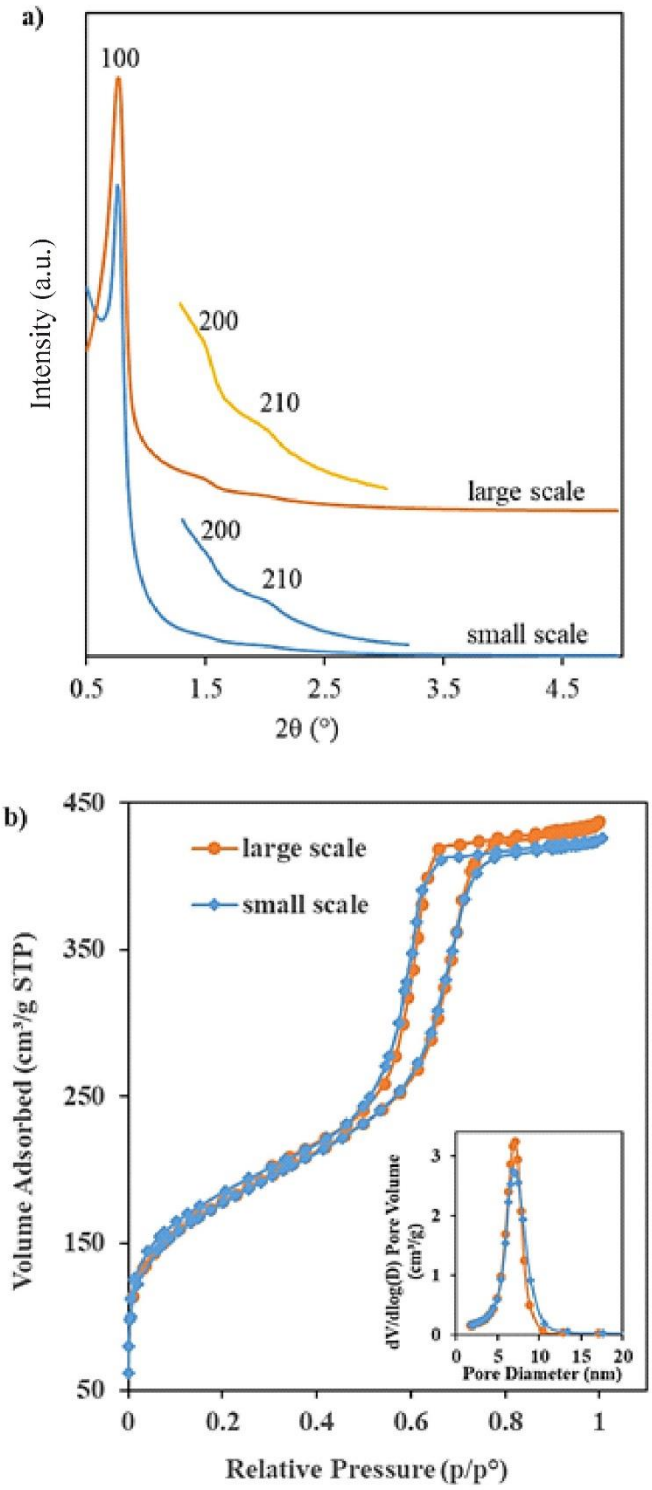

Fig. 10 - a) SAXRD patterns and b) Nitrogen sorption isotherms with pore size distributions (inset) of samples made at small and large (× 25) scale.

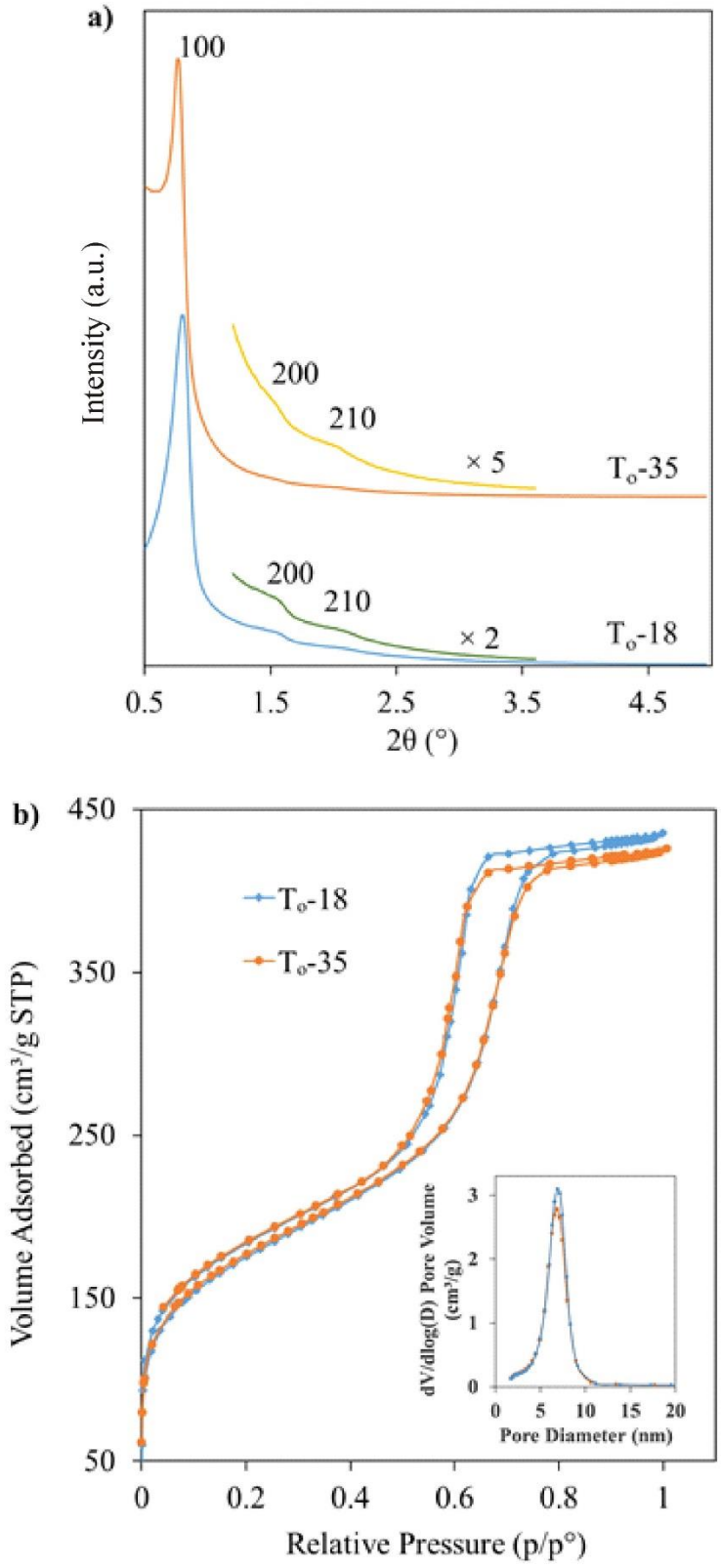

Fig. 11 - a) SAXRD patterns and b) Nitrogen sorption isotherms with pore size distributions (inset) of samples made using the oligermerisation temperatures, T_o, indicated in the figure.

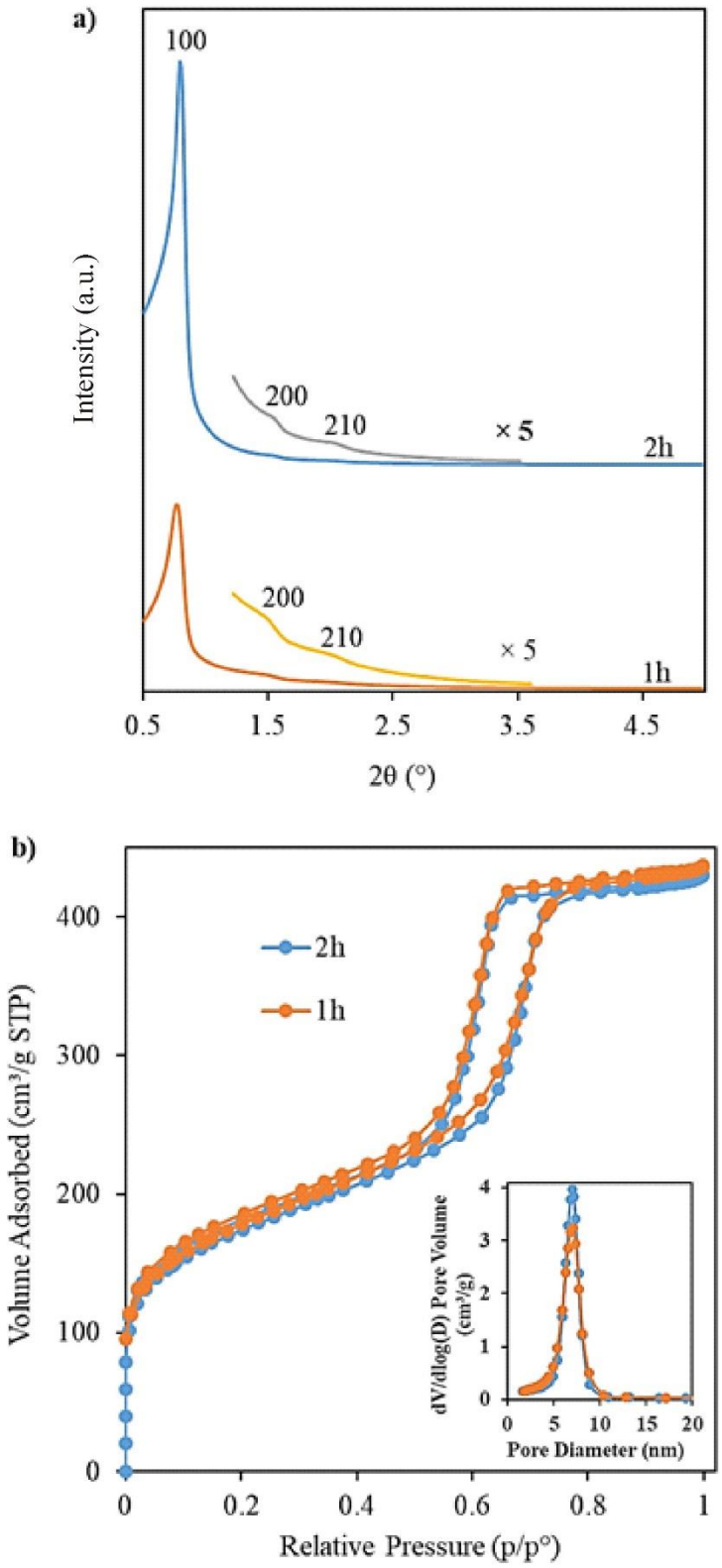

Fig. 12 - a) SAXRD patterns and b) Nitrogen sorption isotherms with pore size distributions (inset) for samples made using the oligomerisation time, t_o, indicated in the figure.

3.3.3 Effect of T_p and t_p

Two sets of experiments were carried out to study the effect of varying polymerisation temperature, T_p, and polymerisation time, t_p, after adding NH_4OH, on the final mesostructure. In the first set of experiments, T_p was set to 20, 25, 30 or 35 °C and t_p to 1 h. All other reaction parameters were kept constant. **Fig. 13~~a~~** shows the SAXRD patterns of all four resulting samples. It can be seen that samples made using T_p=30 °C and 35° C were highly ordered as their SAXRD patterns show three peaks corresponding to the 100, 200 and 210 planes of the 2D hexagonal mesostructure while samples made at 20 ºC and 25 ºC showed only one, broad peak. **Table 2** presents the time for phase separation and textural parameters for these samples. It was found that by increasing the temperature from 20 ºC to 35 ºC the time for phase separation decreased from more than 7 h to less than 10 min. (**Table 2**). The sample which showed the shortest phase separation time was highly ordered (made at 35 ºC) and the sample which had the longest phase separation time is less ordered (made at 20 ºC). The reason behind this is unclear. **Figure S1 (Supplementary Information)** ~~**Fig. 13b** and **c**~~ and **Table 2** give the nitrogen physisorption data for these samples ~~**(Figure S1, Supplementary Information)**~~ show that all samples have a Type IV isotherm with H1 type hysteresis loop and pore size distributions centred around 6.8-7.0 nm. The values of their specific surface area, pore volume, micropore volume and pore diameter are close to each other (**Table 2)**.

Table 2 - Time for phase separation and N_2 physisorption data of samples made under different conditions.

Sample		T_G (min)	SSA (m^2/g)	V_P (cm^3/g)	V_{micro} (cm^3/g)	Dp (nm)
T_p (°C)	t_p (h)					
20	1	> 420	612	0.61	0.05	6.9
25	1	45	646	0.62	0.05	6.8
30	1	15	620	0.59	0.05	6.8
35	1	8	605	0.61	0.05	7.0
30	0.5	75	559	0.56	0.04	7.1
35	0.5	60	605	0.60	0.05	7.0
40	0.5	10	601	0.61	0.05	7.0

T_G: time for gel formation; SSA: Specific surface area; V_P: Pore volume; V_{micro}: Micropore volume; D_P: Pore diameter

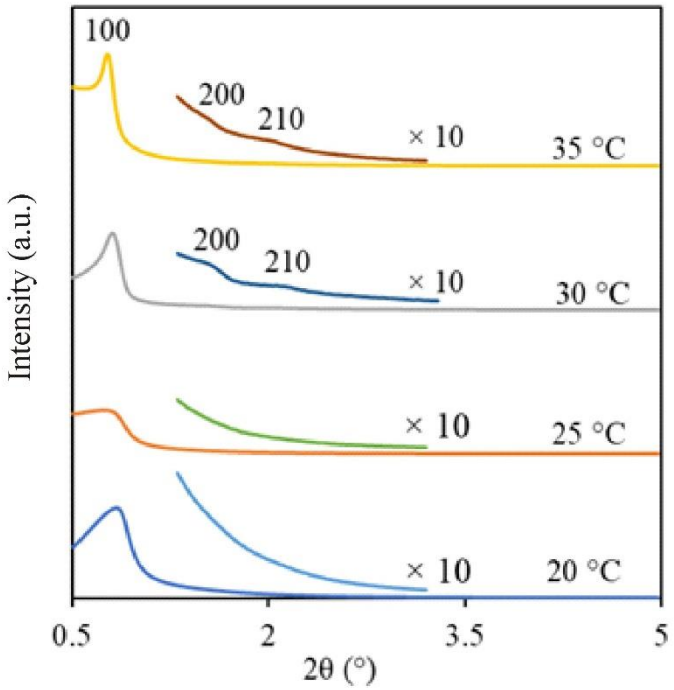

Fig. 13. SAXRD patterns for samples made using the polymerisation temperatures, T_P , indicated in the figure and with polymerisation time, t_p=1 h.

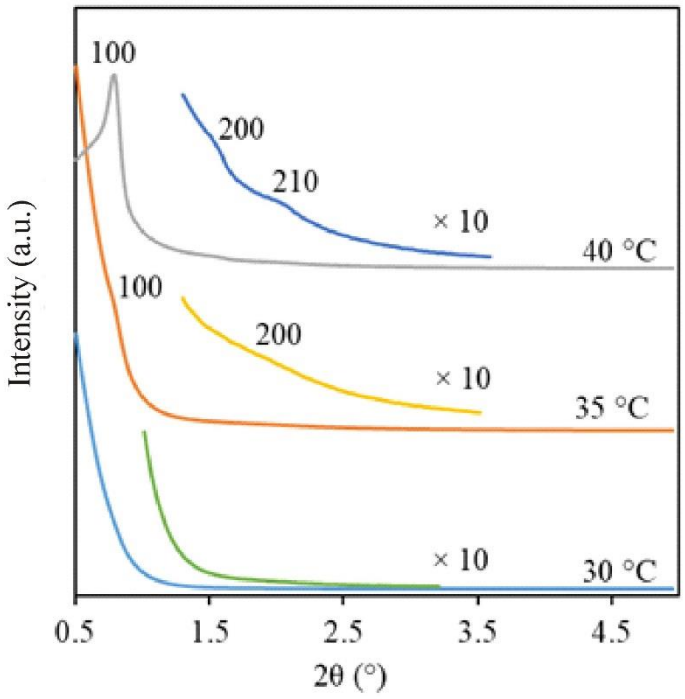

Fig. 14. SAXRD patterns for samples made at the polymerisation temperatures, T_p, indicated in the figure and with a polymerisation time, t_p = 0.5 h.

In a second set of experiments, the effect of T_p was studied for t_p=30 min. The values of T_p selected were 30, 35 and 40 °C. As in the case of t_p=1h, an increase in temperature from 30 to 40 °C resulted in a decrease in phase separation time and an increase in the order of the mesostructure, as can be seen from **Table 2** and **Figure 14**. The SAXRD pattern of the sample made at 40 °C shows three peaks which could be indexed as reflections of 100, 200, and 210 planes of the 2D hexagonal arrangement (**Figure 14a)**. The sample made at 35 °C shows two peaks that correspond to the 100 and 210 planes while the pattern of the sample made at 30 °C does not show any peaks (**Figure 14a)**. All samples gave nitrogen physisorption isotherms of Type IV with H1 type hysteresis loops giving narrow pore size distributions (**Figure S2, Supplementary Information**). **Table 2** shows that there is no significant difference in specific surface area, pore volume and micropore volume between these materials.

The above results indicate that OMCs can be successfully prepared using different combinations of T_p and t_p. When T_p was 40 °C, t_o=30 min. was long enough to make good OMCs while for T_p=30-35 °C t_p=1 h was needed.

3.3.4 Effect of NH_4OH

The amount of the catalyst, NH_4OH, added could affect the rate of polymerisation and hence, possibly, the final mesostructure. To study this, the amount of base added, C_{NH4OH}, was varied from 0.1 to 0.2 mmoles while keeping all other reaction parameters constant.

Figure 15a shows the SAXRD patterns of the four samples made using different C_{NH4OH}. Only the pattern for C_{NH4OH} =0.20 is typical of 2D-hexagonal mesopore structure. This suggests that by decreasing C_{NH4OH} the mesostructure became less ordered. The isotherms of all samples are of Type IV with H1 type hysteresis as is typical of channel-like mesoporous materials and had narrow pore size distributions (**Figure S3, Supplementary Information)**. Other textural parameters such as specific surface area, pore volume, micropore volume, and pore diameter of all samples made using different amounts of NH_4OH were similar to each other (**Table 3**).

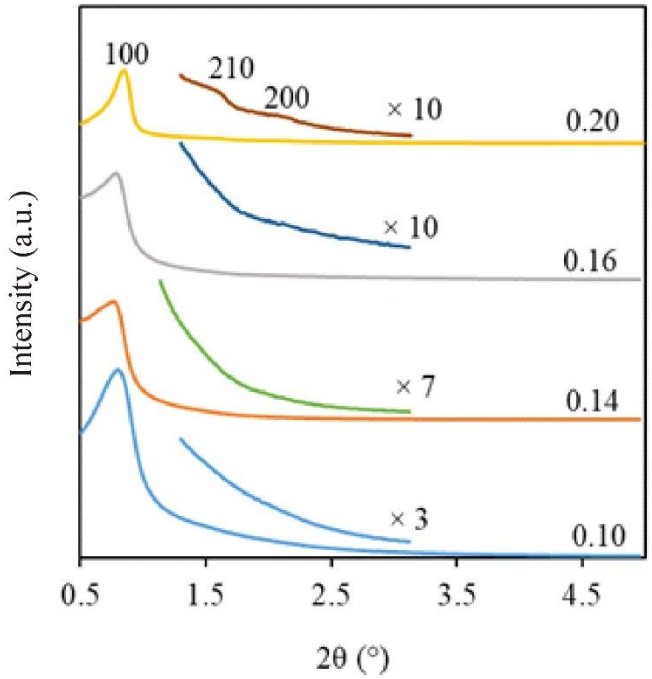

Fig. 15 - SAXRD patterns for samples made using the amounts (in mmoles) of NH_4OH indicated in the figure.

Table 3 - Physisorption data and phase separation time for samples made using the indicated molar additions of NH_4OH, C_{NH4OH}.

C_{NH4OH} (mmoles)	T_G (min)	SSA (m^2/g)	V_P (cm^3/g)	V_{micro} (cm^3/g)	Dp (nm)
0.10	> 120	607	0.59	0.047	6.9
0.14	30	604	0.63	0.047	7.0
0.16	27	614	0.62	0.045	6.8
0.20	8	637	0.61	0.045	6.8

T_G: time for gel formation; SSA: Specific surface area; V_P: Pore volume; V_{micro}: Micropore volume; D_P: Pore diameter

4. Conclusions

Highly ordered metal- and halogen-free OMCs have been successfully synthesised using a reproducible and scalable two-phase method. Particularly because of the absence of metal and halogen ions, which are well-known catalyst poisons, it is expected that these materials will be of interest for use as catalyst supports themselves and also for use as templates for preparation by nanocasting of other non-carbon catalyst materials. Both of these avenues are currently being pursued by the authors.

In this work, NH_4OH plays the role of polymerisation catalyst (replacing e.g. $NaCO_3$) and oxalic acid is the condensation catalyst and aids self-assembly (replacing e.g. HCl). No significant differences in chemical or mesopore structure of the OMCs were observed when using these new catalysts, but there was a slight increase in gel time when using oxalic acid in place of HCl.

T_{calc} plays a major role in determining the final properties of the OMCs. Heating the polymer at 300 ºC is not enough for template removal. The samples calcined at 350 ºC and 400 ºC are polymeric in nature for which reason the adsorption and desorption branches of their physisorption isotherms are not closed and their NMR and FT-IR spectra show significant presence of functional groups. A calcination temperature of 800 ºC marks the complete transformation from polymer to carbon framework. On increasing T_{calc} the shrinkage of the OMCs was pronounced between 350 and 800 ºC and then slowed down at higher temperature. The sample calcined at 600 ºC had the highest surface area of 719 m^2/g. The sample calcined at 1200 °C showed three well defined peaks in the SAXRD pattern showing that the ordered pore structure can resist such high temperatures. This was confirmed in the TEM study.

Varying the oligomerisation temperature, T_o, did not affect the properties of the final mesoporous product but a T_p of 30 ºC or above should be used to obtain ordered mesostructures. The oligomerisation time, t_o should be at least 1 h. Further increase in t_o did not affect the final mesostructure.

5. Acknowledgements

We thank the University of St Andrews for the PhD scholarship of FS. Electron microscopy (EM) was performed at the Electron Microscopy Facility, School of Chemistry, University of St Andrews. We thank Mr Ross Blackley and Dr Daniel Dawson for assistance with EM and NMR analysis, respectively.

References

1 R. Ryoo, S. H. Joo and S. Jun, *J. Phys. Chem. B*, 1999, **103**, 7743–7746.

2 C. Liang, Z. Li and S. Dai, *Angew. Chem. Int. Ed. Engl.*, 2008, **47**, 3696–717.

3 J. Xu, A. Wang and T. Zhang, *Carbon N. Y.*, 2012, **50**, 1807–1816.

4 S. Jun, S. H. Joo, R. Ryoo, M. Kruk, M. Jaroniec, Z. Liu, T. Ohsuna and O. Terasaki, *J. Am. Chem. Soc.*, 2000, **122**, 10712–10713.

5 S.H. Joo, S.J. Choi, I. Oh, J. Kwak, Z. Liu, O. Terasaki, R. Ryoo, *Nature*, **412** (2001), 169-172.

6 F. Zhang, Y. Meng, D. Gu, Z. Chen, B. Tu and D. Zhao, *Chem. Mater.*, 2006, **18**, 5279–5288.

7 M. Li and J. Xue, *J. Colloid Interface Sci.*, 2012, **377**, 169–175.

8 Y. Meng, D. Gu, F. Zhang, Y. Shi, L. Cheng, D. Feng, Z. Wu, Z. Chen, Y. Wan, A. Stein and D. Zhao, *Chem. Mater.*, 2006, **18**, 4447–4464.

9 W. Xin and Y. Song, *RSC Adv.*, 2015, **5**, 83239–83285.

10 T.-Y. Ma, L. Liu and Z.-Y. Yuan, *Chem. Soc. Rev.*, 2013, **42**, 3977–4003.

11 Y. Huang, H. Cai, D. Feng, D. Gu, Y. Deng, B. Tu, H. Wang, P. A. Webley and D. Zhao, *Chem. Commun.*, 2008, 2641.

12 X. Wang, C. Liang and S. Dai, *Langmuir*, 2008, **24**, 7500–5.

13 C. Liu, L. Li, H. Song and X. Chen, *Chem. Commun.*, 2007, **0**, 757–759.

14 D. Walton and P. Lorimer, *Polymers*, Oxford University Press Inc., New York, 2000.

15 G.Gills, *J. Appl. Polym. Sci.*, 1969, **13**, 835–849.

16 R. B. Durairaj, in *Resorcinol*, 2005, pp. 263–339.

17 J. Weber, M. Antonietti and A. Thomas, *Macromolecules*, 2008, **41**, 2880–2885.

18 R. Silverstein, C. Bassler and T. Morril, *Spectrometric identification of organic compounds*, John Wiley & Sons,Inc., New York, Third., 1974.

19 L. Liu, Q.-F. Deng, T.-Y. Ma, X.-Z. Lin, X.-X. Hou, Y.-P. Liu and Z.-Y. Yuan, *J. Mater. Chem.*, 2011, **21**, 16001.